

Supporting Information

From Ce(IO₃)₄ to CeF₂(IO₃)₂: fluorinated homovalent substitution simultaneously enhances SHG response and bandgap for mid-infrared nonlinear optics

Tianhui Wu,[§] Xingxing Jiang,^{‡,§} Chao Wu,^{†,§} Hongyuan Sha,^{ψ,§} Zujian Wang,^ψ Zheshuai Lin,[‡] Zhipeng Huang,[†] Xifa Long,^ψ Mark G. Humphrey,^δ and Chi Zhang^{†,*}

[†] *China-Australia Joint Research Center for Functional Molecular Materials, School of Chemical Science and Engineering, Tongji University, Shanghai 200092, China E-mail: chizhang@tongji.edu.cn*

[‡] *Technical Institute of Physics and Chemistry, Chinese Academy of Sciences, Beijing 100190, China*

^ψ *Key Laboratory of Optoelectronic Materials Chemistry and Physics, State Key Laboratory of Structure Chemistry, Fujian Institute of Research on the Structure of Matter, Chinese Academy of Sciences, Fuzhou, Fujian 350002, China*

^δ *Research School of Chemistry, Australian National University, Canberra, ACT 2601, Australia*

Table of Contents

Table S1. Selected bond distances (\AA) and angles (deg.) for $\text{Ce}(\text{IO}_3)_4$.

Table S2. Selected bond distances (\AA) and angles (deg.) for $\text{CeF}_2(\text{IO}_3)_2$.

Table S3. Atomic coordinates ($\times 10^4$) and equivalent isotropic displacement parameters ($\text{\AA}^2 \times 10^3$) of $\text{Ce}(\text{IO}_3)_4$. $U(\text{eq})$ is defined as one third of the trace of the orthogonalized U_{ij} tensor.

Table S4. Atomic coordinates ($\times 10^4$) and equivalent isotropic displacement parameters ($\text{\AA}^2 \times 10^3$) of $\text{CeF}_2(\text{IO}_3)_2$. $U(\text{eq})$ is defined as one third of the trace of the orthogonalized U_{ij} tensor.

Figure S1. Experimental and simulated powder X-ray diffraction patterns of $\text{Ce}(\text{IO}_3)_4$ (a) and $\text{CeF}_2(\text{IO}_3)_2$ (b).

Figure S2. SEM images of $\text{Ce}(\text{IO}_3)_4$ (a) and $\text{CeF}_2(\text{IO}_3)_2$ (b) and their elemental distribution maps.

Figure S3. Thermogravimetric analyses of $\text{CeF}_2(\text{IO}_3)_2$ under a N_2 atmosphere.

Figure S4. Asymmetric units of $\text{Ce}(\text{IO}_3)_4$ (a) and $\text{CeF}_2(\text{IO}_3)_2$ (b).

Figure S5. Infrared spectra of $\text{Ce}(\text{IO}_3)_4$ (a) and $\text{CeF}_2(\text{IO}_3)_2$ (b).

Figure S6. UV-Vis-NIR diffuse absorption spectra of $\text{Ce}(\text{IO}_3)_4$ (a) and $\text{CeF}_2(\text{IO}_3)_2$ (b). The inset shows the corresponding band gap.

Figure S7. Comparison of (a) the original $\text{Ce}(\text{IO}_3)_4$ crystal and (b) the $\text{Ce}(\text{IO}_3)_4$ crystal achieving complete extinction.

Figure S8. Photograph of the crystal size of $\text{Ce}(\text{IO}_3)_4$ (a) and $\text{CeF}_2(\text{IO}_3)_2$ (b).

Figure S9. Calculated band structures of $\text{Ce}(\text{IO}_3)_4$ (a) and $\text{CeF}_2(\text{IO}_3)_2$ (b).

Figure S10. Calculated wavelength-dependent refractive indices of $\text{Ce}(\text{IO}_3)_4$.

Table S1. Selected bond distances (Å) and angles (deg.) for Ce(IO₃)₄^[a].

Ce(1)-O(2)#1	2.298(9)	O(1)-Ce(1)-O(7)	124.1(2)
Ce(1)-O(4)	2.309(7)	O(5)-Ce(1)-O(7)	132.3(3)
Ce(1)-O(1)	2.360(6)	O(9)-Ce(1)-O(7)	144.6(2)
Ce(1)-O(5)	2.361(7)	O(2)#1-Ce(1)-O(11)	135.9(3)
Ce(1)-O(9)	2.381(6)	O(4)-Ce(1)-O(11)	95.0(3)
Ce(1)-O(7)	2.385(7)	O(1)-Ce(1)-O(11)	70.7(2)
Ce(1)-O(11)	2.410(6)	O(5)-Ce(1)-O(11)	144.1(2)
Ce(1)-O(10)	2.427(6)	O(9)-Ce(1)-O(11)	80.6(3)
I(1)-O(3)	1.774(8)	O(7)-Ce(1)-O(11)	73.9(3)
I(1)-O(2)	1.809(9)	O(2)#1-Ce(1)-O(10)	65.2(3)
I(1)-O(1)	1.810(6)	O(4)-Ce(1)-O(10)	140.9(2)
I(2)-O(6)	1.805(7)	O(1)-Ce(1)-O(10)	131.6(2)
I(2)-O(5)#2	1.815(8)	O(5)-Ce(1)-O(10)	134.0(2)
I(2)-O(4)	1.818(7)	O(9)-Ce(1)-O(10)	77.7(2)
I(3)-O(8)	1.770(7)	O(7)-Ce(1)-O(10)	71.2(2)
I(3)-O(7)	1.815(6)	O(11)-Ce(1)-O(10)	71.6(2)
I(3)-O(9)#3	1.836(6)	O(3)-I(1)-O(2)	100.9(6)
I(4)-O(12)	1.787(7)	O(3)-I(1)-O(1)	97.6(3)
I(4)-O(10)	1.816(6)	O(2)-I(1)-O(1)	90.3(3)
I(4)-O(11)#4	1.820(6)	O(6)-I(2)-O(5)#2	97.7(3)
O(2)-Ce(1)#5	2.298(9)	O(6)-I(2)-O(4)	98.2(3)
O(5)-I(2)#6	1.815(8)	O(5)#2-I(2)-O(4)	98.0(4)
O(9)-I(3)#7	1.836(6)	O(8)-I(3)-O(7)	97.9(4)
O(11)-I(4)#8	1.820(6)	O(8)-I(3)-O(9)#3	97.8(3)
		O(7)-I(3)-O(9)#3	95.8(3)
O(2)#1-Ce(1)-O(4)	124.2(4)	O(12)-I(4)-O(10)	97.7(3)
O(2)#1-Ce(1)-O(1)	135.8(4)	O(12)-I(4)-O(11)#4	99.9(4)
O(4)-Ce(1)-O(1)	71.8(2)	O(10)-I(4)-O(11)#4	94.7(3)
O(2)#1-Ce(1)-O(5)	71.3(3)	I(1)-O(1)-Ce(1)	126.7(3)
O(4)-Ce(1)-O(5)	77.5(3)	I(1)-O(2)-Ce(1)#5	132.2(5)
O(1)-Ce(1)-O(5)	73.6(3)	I(2)-O(4)-Ce(1)	132.3(4)
O(2)#1-Ce(1)-O(9)	81.9(4)	I(2)#6-O(5)-Ce(1)	150.0(4)
O(4)-Ce(1)-O(9)	137.8(2)	I(3)-O(7)-Ce(1)	139.5(4)
O(1)-Ce(1)-O(9)	67.2(2)	I(3)#7-O(9)-Ce(1)	138.1(4)
O(5)-Ce(1)-O(9)	81.9(3)	I(4)-O(10)-Ce(1)	135.7(3)
O(2)#1-Ce(1)-O(7)	99.5(4)	I(4)#8-O(11)-Ce(1)	132.3(3)
O(4)-Ce(1)-O(7)	69.8(2)		

^[a] Symmetry codes for Ce(IO₃)₄: #1 x, x-y+1, z-1/2; #2 -y, x-y+1, z; #3 -y-1/3, -x-2/3, z-1/6; #4 -y-2/3, x-y+2/3, z-1/3; #5 x, x-y+1, z+1/2; #6 -x+y-1, -x, z; #7 -y-2/3, -x-1/3, z+1/6; #8 -x+y-4/3, -x-2/3, z+1/3.

Table S2. Selected bond distances (Å) and angles (deg.) for CeF₂(IO₃)₂ [a].

Ce(1)-F(2)	2.109(4)	O(4)-Ce(1)-O(3)	79.95(18)
Ce(1)-F(1)	2.198(3)	F(2)-Ce(1)-O(5)#3	138.88(14)
Ce(1)-F(1)#1	2.229(3)	F(1)-Ce(1)-O(5)#3	134.60(15)
Ce(1)-O(1)#2	2.314(5)	F(1)#1-Ce(1)-O(5)#3	69.12(15)
Ce(1)-O(4)	2.314(4)	O(1)#2-Ce(1)-O(5)#3	72.28(17)
Ce(1)-O(3)	2.413(5)	O(4)-Ce(1)-O(5)#3	69.23(16)
Ce(1)-O(5)#3	2.510(4)	O(3)-Ce(1)-O(5)#3	68.49(14)
Ce(1)-O(2)#4	2.568(4)	F(2)-Ce(1)-O(2)#4	71.17(15)
Ce(1)-O(6)#5	2.814(5)	F(1)-Ce(1)-O(2)#4	71.16(16)
O(1)-I(1)	1.811(4)	F(1)#1-Ce(1)-O(2)#4	138.20(15)
O(1)-Ce(1)#6	2.314(5)	O(1)#2-Ce(1)-O(2)#4	68.30(17)
I(1)-O(2)	1.784(4)	O(4)-Ce(1)-O(2)#4	71.79(18)
I(1)-O(3)	1.836(4)	O(3)-Ce(1)-O(2)#4	139.88(15)
F(1)-Ce(1)#7	2.229(3)	O(5)#3-Ce(1)-O(2)#4	123.45(16)
O(2)-Ce(1)#8	2.568(4)	F(2)-Ce(1)-O(6)#5	66.33(15)
I(2)-O(6)	1.794(5)	F(1)-Ce(1)-O(6)#5	66.94(13)
I(2)-O(4)	1.810(4)	F(1)#1-Ce(1)-O(6)#5	65.09(13)
I(2)-O(5)	1.809(4)	O(1)#2-Ce(1)-O(6)#5	137.25(14)
O(6)-Ce(1)#9	2.814(5)	O(4)-Ce(1)-O(6)#5	132.78(16)
O(5)-Ce(1)#10	2.510(4)	O(3)-Ce(1)-O(6)#5	61.78(14)
		O(5)#3-Ce(1)-O(6)#5	115.29(15)
F(2)-Ce(1)-F(1)	85.49(15)	O(2)#4-Ce(1)-O(6)#5	121.23(15)
F(2)-Ce(1)-F(1)#1	76.44(15)	I(1)-O(1)-Ce(1)#6	139.3(2)
F(1)-Ce(1)-F(1)#1	132.01(3)	O(2)-I(1)-O(1)	97.7(2)
F(2)-Ce(1)-O(1)#2	81.14(17)	O(2)-I(1)-O(3)	96.4(2)
F(1)-Ce(1)-O(1)#2	139.46(16)	O(1)-I(1)-O(3)	95.2(2)
F(1)#1-Ce(1)-O(1)#2	81.37(15)	Ce(1)-F(1)-Ce(1)#7	172.6(2)
F(2)-Ce(1)-O(4)	142.62(18)	I(1)-O(2)-Ce(1)#8	144.8(3)
F(1)-Ce(1)-O(4)	78.08(16)	O(6)-I(2)-O(4)	99.5(2)
F(1)#1-Ce(1)-O(4)	138.15(17)	O(6)-I(2)-O(5)	102.70(19)
O(1)#2-Ce(1)-O(4)	89.87(17)	O(4)-I(2)-O(5)	97.5(2)
F(2)-Ce(1)-O(3)	128.10(15)	I(1)-O(3)-Ce(1)	131.5(2)
F(1)-Ce(1)-O(3)	75.63(15)	I(2)-O(6)-Ce(1)#9	118.1(2)
F(1)#1-Ce(1)-O(3)	81.43(15)	I(2)-O(5)-Ce(1)#10	137.5(2)
O(1)#2-Ce(1)-O(3)	140.58(16)	I(2)-O(4)-Ce(1)	139.2(2)

[a] Symmetry codes for CeF₂(IO₃)₂: #1 x-1/2, -y+3/2, z; #2 -x+1/2, y-1/2, z-1/2; #3 x-1/2, -y+1/2, z; #4 -x+1, -y+1, z-1/2; #5 x, y+1, z; #6 -x+1/2, y+1/2, z+1/2; #7 x+1/2, -y+3/2, z; #8 -x+1, -y+1, z+1/2; #9 x, y-1, z; #10 x+1/2, -y+1/2, z.

Table S3. Atomic coordinates ($\times 10^4$) and equivalent isotropic displacement parameters ($\text{\AA}^2 \times 10^3$) of $\text{Ce}(\text{IO}_3)_4$. $U(\text{eq})$ is defined as one third of the trace of the orthogonalized U_{ij} tensor.

Atom	x	y	z	$U_{\text{eq}}(\text{\AA}^2)$	BVS
Ce(1)	-5319(1)	1681(1)	3286(1)	12(1)	3.22
I(1)	-5319(1)	2171(1)	5677(1)	17(1)	5.19
I(2)	-3705(1)	1535(1)	3822(1)	21(1)	4.98
I(3)	-5042(1)	430(1)	1403(1)	13(1)	5.07
I(4)	-6950(1)	36(1)	2053(1)	14(1)	5.05
O(1)	-5410(3)	1829(4)	5068(5)	20(1)	2.08
O(2)	-5368(7)	2400(7)	6810(7)	70(4)	1.98
O(3)	-6644(5)	1353(4)	6062(8)	47(2)	2.03
O(4)	-4288(4)	1884(4)	4062(6)	31(2)	1.86
O(5)	-4731(4)	2906(4)	3583(6)	32(2)	1.98
O(6)	-3527(4)	1421(4)	5143(6)	31(2)	2.10
O(7)	-4940(4)	925(4)	2572(5)	26(2)	1.94
O(8)	-4143(4)	832(4)	1061(7)	32(2)	2.06
O(9)	-6319(3)	1782(4)	3716(5)	24(1)	2.16
O(10)	-6182(3)	912(3)	2033(4)	18(1)	1.69
O(11)	-6040(4)	547(3)	4073(5)	24(1)	1.78
O(12)	-6506(4)	-449(4)	1845(6)	34(2)	1.84

Table S4. Atomic coordinates ($\times 10^4$) and equivalent isotropic displacement parameters ($\text{\AA}^2 \times 10^3$) of $\text{CeF}_2(\text{IO}_3)_2$. $U(\text{eq})$ is defined as one third of the trace of the orthogonalized U_{ij} tensor.

Atom	x	y	z	$U_{\text{eq}}(\text{\AA}^2)$	BVS
Ce(1)	3244(1)	6202(1)	3964(1)	6(1)	3.74
I(1)	2985(1)	6646(1)	7241(1)	7(1)	5.02
I(2)	4246(1)	1299(1)	5401(1)	8(1)	5.09
F(1)	5785(4)	7335(5)	4032(4)	15(1)	1.10
F(2)	3087(4)	7638(6)	2388(4)	18(1)	0.73
O(1)	3288(6)	8921(6)	7979(5)	14(1)	2.13
O(2)	4977(6)	5628(7)	7510(4)	20(1)	2.02
O(3)	3469(5)	7616(6)	5829(4)	11(1)	1.91
O(4)	4626(6)	3738(6)	4901(5)	15(1)	2.13
O(5)	6365(5)	452(6)	5357(4)	14(1)	1.95
O(6)	3372(5)	266(7)	4139(4)	13(1)	1.86

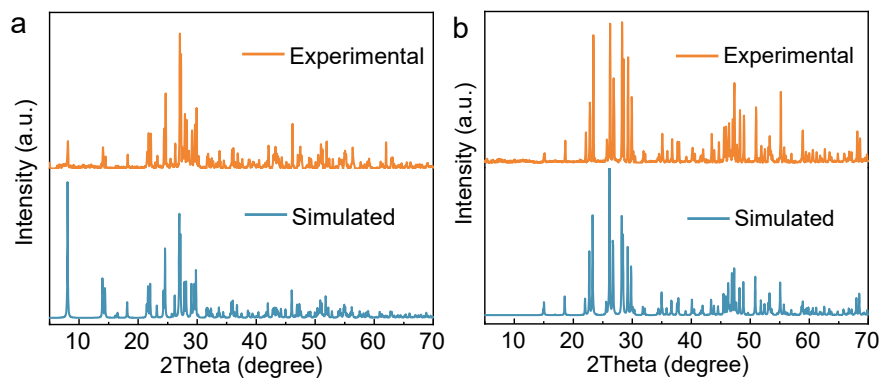


Figure S1. Experimental and simulated powder X-ray diffraction patterns of $\text{Ce}(\text{IO}_3)_4$ (a) and $\text{CeF}_2(\text{IO}_3)_2$ (b).

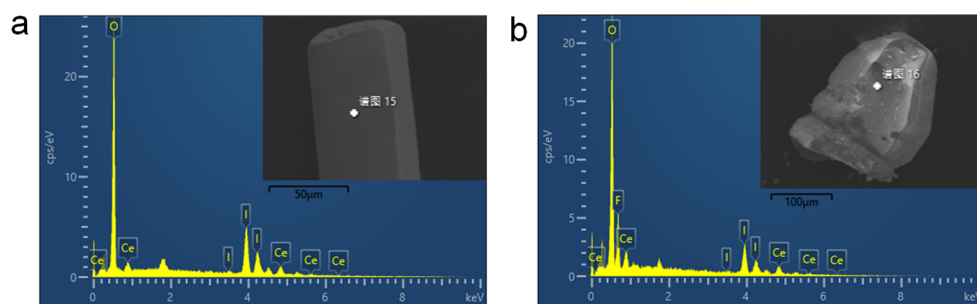


Figure S2. SEM images of $\text{Ce}(\text{IO}_3)_4$ (a) and $\text{CeF}_2(\text{IO}_3)_2$ (b) and their elemental distribution maps.

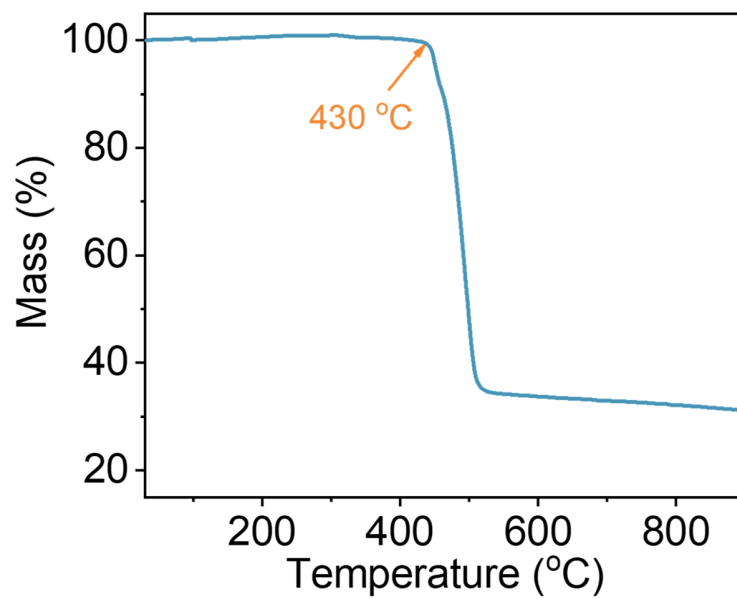


Figure S3. Thermogravimetric analyses of $\text{CeF}_2(\text{IO}_3)_2$ under a N_2 atmosphere.

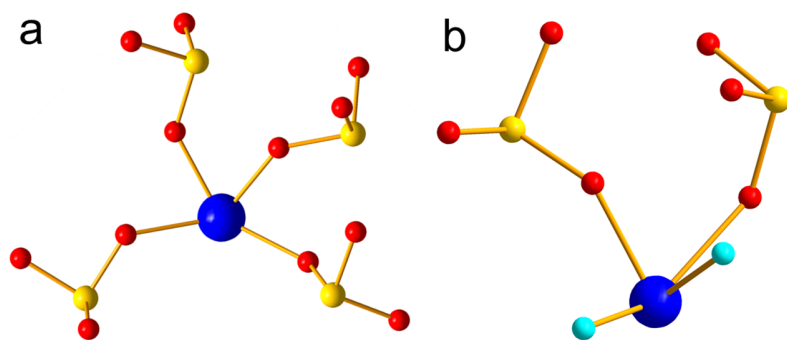


Figure S4. Asymmetric units of $\text{Ce}(\text{IO}_3)_4$ (a) and $\text{CeF}_2(\text{IO}_3)_2$ (b).

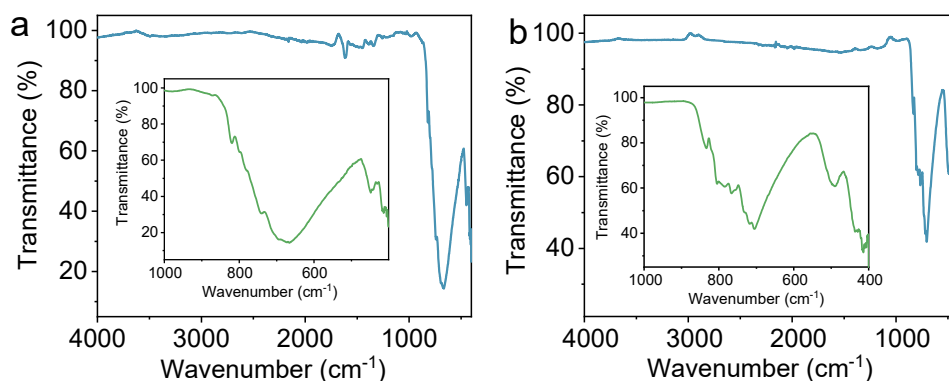


Figure S5. Infrared spectra of $\text{Ce}(\text{IO}_3)_4$ (a) and $\text{CeF}_2(\text{IO}_3)_2$ (b).

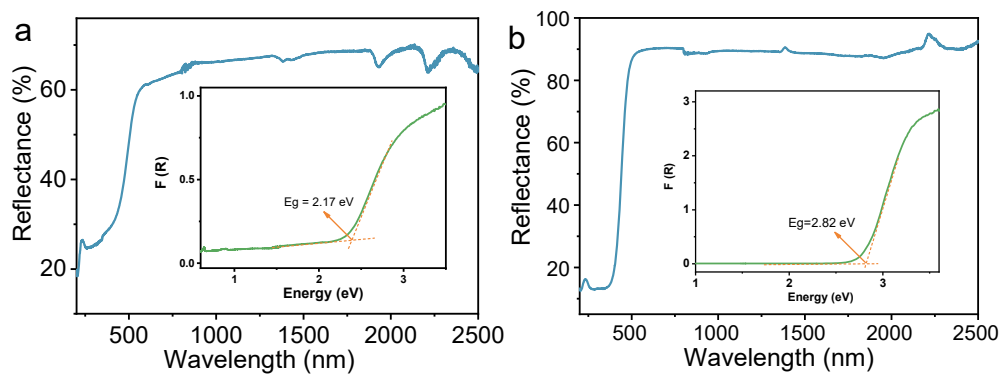


Figure S6. UV-Vis-NIR diffuse reflectance spectra of $\text{Ce}(\text{IO}_3)_4$ (a) and $\text{CeF}_2(\text{IO}_3)_2$ (b). The inset shows the corresponding band gap.

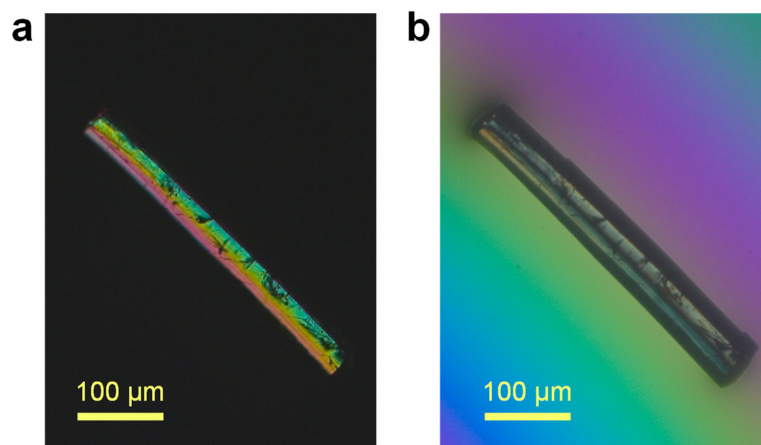


Figure S7. Comparison of (a) the original Ce(IO₃)₄ crystal and (b) the Ce(IO₃)₄ crystal achieving complete extinction.

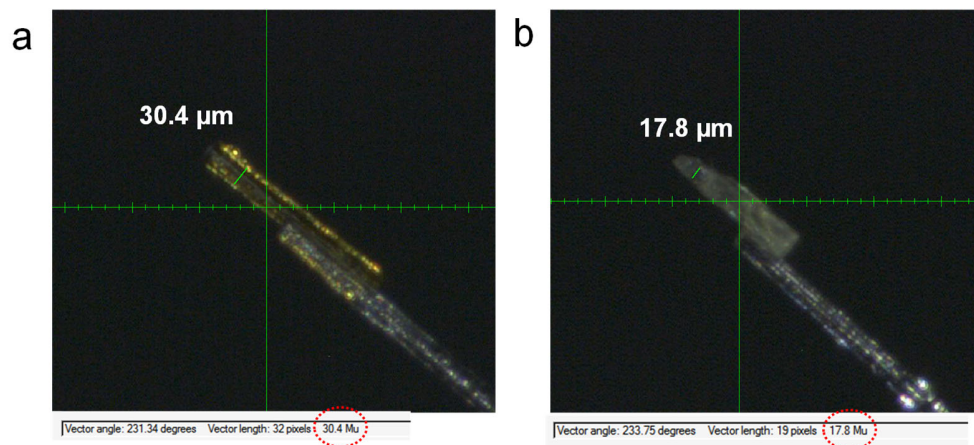


Figure S8. Photograph of the crystal size of $\text{Ce}(\text{IO}_3)_4$ (a) and $\text{CeF}_2(\text{IO}_3)_2$ (b).

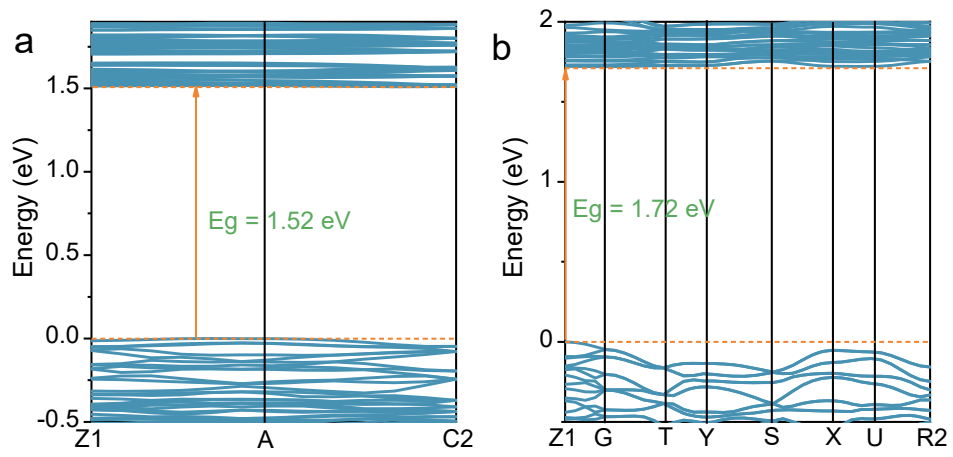


Figure S9. Calculated band structures of $\text{Ce}(\text{IO}_3)_4$ (a) and $\text{CeF}_2(\text{IO}_3)_2$ (b).

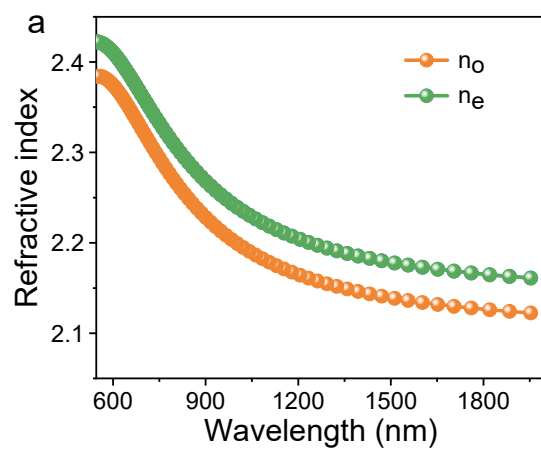


Figure S10. Calculated wavelength-dependent refractive indices of $\text{Ce}(\text{IO}_3)_4$.